Climatic Change (2015) 129:281–294
DOI 10.1007/s10584-015-1334-1

Incorporating uncertainty of groundwater modeling in sea-level rise assessment: a case study in South Florida

Hannah M. Cooper · Caiyun Zhang · Donna Selch

Received: 16 October 2014 / Accepted: 12 January 2015 / Published online: 30 January 2015

Abstract Researchers can assist in effective decision making by reducing uncertainty in marine and groundwater inundation due to Sea-level Rise (SLR). A majority of studies consider marine inundation, but only recently has groundwater inundation been incorporated into the SLR mapping. However, the effect of including uncertainty in groundwater modeling is still not well understood. In this study, we evaluate the effect of considering groundwater modeling uncertainty in assessing land area inundated vulnerable to marine and groundwater inundation in South Florida. Six Water Table Elevation Model (WTEM) techniques (Multiple Linear Regression (MLR), Geographic Weighted Regression (GWR), Global Polynomial Interpolation (GPI), Inverse Distance Weighted (IDW), Ordinary Kriging (OK), and Empirical Bayesian Kriging (EBK)) are tested to identify the best approach. Simple inundation models excluding uncertainty with and without WTEM are examined. Refined inundation models using Monte Carlo simulation that include uncertainty in future SLR estimates, LiDAR elevation, vertical datums and the transformations made between datums with and without WTEM uncertainty are evaluated. GPI and EBK are recognized as the best for producing WTEMs in two primary physiographic regions (the Southern Slope and Atlantic Coastal Ridge). Excluding uncertainty without WTEM underestimates total land area by 14 %, while including uncertainty without WTEM overestimates total vulnerable land area by 16 % at the 95 % probability threshold. It is significant to include WTEM uncertainty in SLR vulnerability analysis for more effective adaptation decisions.

1 Introduction

South Florida is one of the most vulnerable regions to sea-level rise (SLR) due to low elevations and gentle slopes characterizing coastal areas that support human populations and natural ecosystems. The Intergovernmental Panel on Climate Change (IPCC) Fifth Assessment Report Representative Concentration Pathway (RCP) 8.5 scenario predicts a median value of 74 cm global SLR by 2100 (Church et al. 2013). In order to adapt to these future conditions, the spatial distribution of potential effects should be assessed through SLR vulnerability mapping which serves as important decision-support tools (Cooper et al. 2013). It is preferable to consider uncertainty in the underlying data to better ensure the reliability of these planning

H. M. Cooper (✉) · C. Zhang · D. Selch
Department of Geosciences, Florida Atlantic University, Boca Raton, FL 33431, USA
e-mail: hcooper2013@fau.edu

tools (e.g., Purvis et al. 2008; Gesch 2009). Researchers can assist in effective decision making by reducing uncertainty in both types of flooding due to SLR: marine and groundwater inundation.

SLR vulnerability applications frequently aim to reduce error in marine inundation using Light Detection and Ranging (LiDAR) derived Digital Elevation Models (DEMs). LiDAR elevation measurements are more accurate when they have a smaller measurement error (e.g., the distribution of error in the dataset is 6 cm σ opposed to 20 cm σ). Although the horizontal error is important, LiDAR DEM is typically defined by vertical error quantified by Federal Geographic Data Committee (FGDC) National Standards for Spatial Data Accuracy (NSSDA) statistical procedures as Root Mean Square Error (RMSE) and Linear Error (LE) at 95 % confidence interval (RMSE×1.96) (FGDC 1998). This led to the approach where the LE is added to the inundation boundary to define an additional zone of uncertainty (e.g., Gesch 2009; Cooper et al. 2012). However, these efforts were limited by exclusion of other quantifiable uncertainties related to LiDAR DEM. For example, there are errors in the datum to which LiDAR DEM is vertically referenced (e.g., orthometric datum North American Vertical Datum of 1988 (NAVD 88) and tidal datum Mean Higher High Water (MHHW)). Additionally, there are errors in the process of transforming LiDAR DEMs from NAVD 88 to MHHW. A number of efforts have been successful at combining errors in LiDAR DEM, datums, and transformations made between datums using either the LE approach (e.g. Gesch 2013) or a modified z-score approach that subtracts the elevation at a grid cell from a specific SLR scenario divided by all errors combined (e.g., Mitsova et al. 2012; Schmid et al. 2013; Kane et al. 2014). These approaches are also known to have their challenges; they require errors not to be correlated and follow a Gaussian distribution with zero bias. On the other hand, this is not the case for a Monte Carlo approach where a random variable is sampled from an array of probability distributions. Application of the Monte Carlo approach allows for the range of uncertainty in future SLR estimates (not assumed Gaussian) to be incorporated into the vulnerability mapping (Purvis et al. 2008) along with error in LiDAR DEM and vertical datums (Cooper and Chen 2013). Another approach applied regression-kriging to model elevation errors for input in Monte Carlo simulation (Leon et al. 2014). However, it is important to note one major drawback to all these efforts: groundwater modeling is excluded.

Compared to marine inundation modeling, research in groundwater inundation modeling is relatively scarce. Water Table Elevation Models (WTEMs) have recently been used to model groundwater inundation by assuming a linear increase in groundwater with SLR (e.g., Rotzoll and Fletcher 2012; Masterson et al. 2013; Manda et al. 2014). WTEMs are commonly generated from observed Water Table Elevations (WTEs) through modeling techniques (e.g., Sepulveda 2003; Sun et al. 2009; Chung and Rogers 2012; Zhu et al. 2013; Rotzoll and Fletcher 2012; Manda et al. 2014; Marrack 2014; Yao et al. 2014). The Multiple Linear Regression (MLR) model assumes relationships being measured between a dependent variable and independent variables is stationary (i.e., global parameter estimates are applied equally over space) (Fotheringham et al. 1998). Some researchers used DEMs (e.g., Sepulveda 2003; Chung and Rogers 2012) or distance of WTE from the ocean (Rotzoll and Fletcher 2012; Marrack 2014) as auxiliary information in the models. The Geographic Weighted Regression (GWR) approach assumes relationships being measured between a dependent variable and independent variables exhibit non-stationary characteristics (local parameter estimates vary over space) (Fotheringham et al. 1998), which may also be useful for WTEM generation. The Global Polynomial Interpolation (GPI) method is a trend surface analysis where the distribution of observational data is described by two-dimensional polynomial equation of first, second or higher degree (Yao et al. 2014). The Inverse Distance Weighted (IDW) approach estimates elevations at unknown locations by using a distance-weighted sum of known elevations in a

surrounding neighborhood (Sun et al. 2009). The widely used Kriging approach predicts unknown elevations from observed data at known locations by employing a variogram (Sun et al. 2009). Various Kriging procedures have been used such as Ordinary Kriging (OK) that requires manual adjustments to parameters, and Empirical Bayesian Kriging (EBK) that automates the process and considers uncertainty in the covariance function (Qian 1997). All these modeling techniques have their specific pros and cons and there is no universal approach used to generating WTEM. Therefore, we test various methods to determine which approach provides WTEM with best vertical accuracy for use in groundwater inundation assessment for our study area.

As it is preferable to consider uncertainty in future SLR estimates, LiDAR DEM, vertical datums and transformations made between datums, the uncertainty in WTEM should also be considered. Incorporating the uncertainty in WTEM would add to the integrity of SLR mapping planning tools. However, no studies to date include uncertainty in groundwater modeling. The objectives of this study are threefold: 1) to determine which approaches produce WTEM with best vertical accuracy for the study area; 2) to evaluate the effect of excluding uncertainty with and without WTEM to calculate land area vulnerable to marine and groundwater inundation; and 3) to evaluate the effect of including uncertainty in future SLR estimates, LiDAR DEM, vertical datums, transformations made between datums, with and without WTEM uncertainty on calculating land area vulnerable to marine and groundwater inundation. The following section introduces the study area and data. Section 3 first presents methods to generating WTEM and accuracy assessment, and second to combining vertical uncertainties and modeling inundation. Section 4 reports results and discussion. Section 5 presents conclusions and future research.

2 Study area and data

2.1 Study area

Our study site is located in southeast Miami-Dade County, Florida with an area of approximate 925 km^2, where WTEMs are required for groundwater inundation modeling (Fig. 1). The area consists of wetlands, estuaries, and coastal ecosystems including a portion of Everglades National Park, agricultural and urban areas. This study is limited to current water management practices that include a highly managed system of canals, operational structures, and levees that modify the natural environment (marshlands) to meet human needs. The canal system is gravity flow based and consists of primary and secondary canals. The primary canals include natural water courses providing drainage basin flows to the ocean or major water bodies inland, and the secondary canals control surface and groundwater levels and runoff that discharge into primary canals and natural waterways (Giddings et al. 2006). The stage in a canal highly determines groundwater elevation (SFWMD 2014). The Biscayne aquifer, an unconfined aquifer dominantly limestone and highly permeable (e.g., Giddings et al. 2006), underlies the study area. The nearest weather station is Miami International Airport. Monthly precipitation averaged from 1995 to 2005 during the wet season (May – October) demonstrated the best indicator of peak groundwater levels was September (28 cm). Therefore, we produced WTEMs using September water level data. Groundwater and surface water levels range −0.13 m to 1.59 m above NAVD 88, as identified from WTE observations (Fig. 1). Land elevation ranges −2.4 m below to 45.7 m above NAVD 88, as identified from the LiDAR DEM. Within the study area, Florida's two most southern mainland cities, Homestead and Florida City, are chosen to model potential marine and groundwater inundation due to SLR.

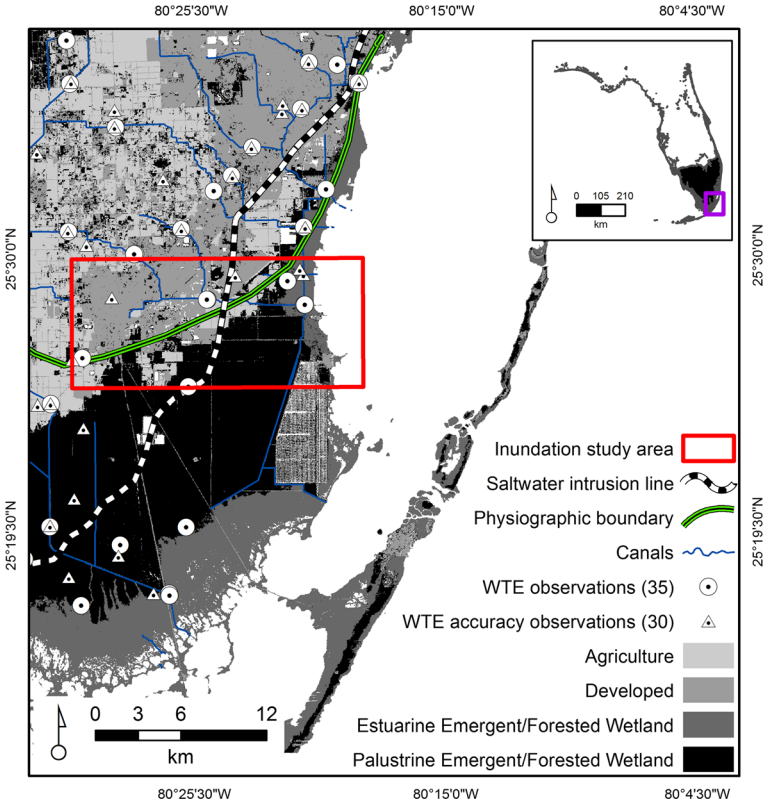

Fig. 1 Location of study area in southeast Miami-Dade County, Florida. WTE = Water Table elevation; physiographic boundary divides Atlantic coastal ridge to north, and Southern slope to south

2.2 Data

Data used in this study include physiographic region boundaries, LiDAR DEM, and time series of WTE observations. First, physiographic regions defined by White (1970) were obtained from Southwest Florida Water Management District. Physiographic regions are useful for defining WTEM boundaries because they often distinguish hydrologic regions within low elevations such as in Florida (Sepulveda 2003). The two primary physiographic regions within the study area include the Atlantic Coastal Ridge and Southern Slope (see Fig. 1). The LiDAR DEM was obtained from South Florida Water Management District (SFWMD). The State of Florida Division of Emergency Management collected the topographic LiDAR data in August 2007 for the study area. The vendor post-processed the LiDAR into ground and non-ground returns using proprietary software. The maximum post spacing reported is 1.2 m for unobscured areas. Ground returns and hydrographic breaklines were used by SFWMD to generate the 3 m resolution LiDAR DEM. SFWMD followed National Digital Elevation Program (NDEP 2004) guidelines to test Fundamental Vertical Accuracy (FVA) of the LiDAR DEM using 308 GPS-derived ground control points collected by the vendor. The RMSE of 6.5 cm is limited to FVA, which likely underestimates LiDAR error in some areas of this study because LiDAR errors are noted to be larger over marsh areas (Schmid et al. 2011).

WTE observations were obtained from the hydrometeorologic, water quality, and hydrogeologic data storage and retrieval system produced by SFWMD in collaboration with agencies such as U.S. Geological Survey (USGS) and Everglades National Park (http://www.sfwmd.gov/dbhydro). A total of 65 observations of daily mean time-series data averaged as monthly values for September from 1995 to 2005 were obtained for generating WTEM and accuracy assessment. WTEs were vertically referenced to National Geodetic Vertical Datum of 1929 (NGVD 29). Transformations from NGVD 29 to NAVD 88 were made for this study using NOAA and National Geodetic Survey datum transformation model VERTCON (http://www.ngs.noaa.gov/PC_PROD/VERTCON/), which computes the modeled difference in orthometric height between NAVD 88 and NGVD 29 for a given x, y coordinate. The uncertainties in NGVD 29, NAVD 88 and the transformation made between them were included in this study. WTEs referenced to NGVD 29 were found on average 47 cm below NAVD 88. Once WTE values were obtained, several approaches were tested to determine the best model in producing WTEM for the study site.

3 Methods

3.1 Water Table Elevation Model (WTEM) generation

Not all 65 WTE observations were considered when generating WTEMs. In order to reflect the distribution of error in a dataset, a minimum of 20 check points is recommended (FGDC 1998). In this study a total of 30 WTEs were randomly selected from the 65 monitoring points for accuracy assessment. The remaining 35 WTEs were used to create WTEMs: 20 for Atlantic Coastal Ridge and 15 for Southern Slope, respectively.

A total of six approaches were employed in ESRI's ArcGIS and tested to determine which could provide WTEMs with best vertical accuracy. It is important to note all parameters were chosen based on trial and error that gave best results for our particular datasets and study area. First, the MLR approach by Sepulveda (2003) was utilized and extended to GWR in this study. The MLR approach accounted for when the water table is not mimicked by land elevation such as areas of high hydraulic conductivity (e.g., Biscayne aquifer; Fish and Stewart 1991) by creating a Minimum Water Table Elevation (MINWTE) surface from elevations of lakes and linearly interpolated river stages. Due to South Florida's unique system of canals, canal stage was computed by interpolating linearly between measured z or elevation values of canal heads and tails using the following equation:

$$Canal = \left(\frac{Canal_{tail,z} - Canal_{head,z}}{d_{tail}}\right) d_{x,y} + Canal_{head,z} \quad (1)$$

where $Canal_{tail,z}$ is the measured z at the tail, $Canal_{head,z}$ is the measured z at the head, d_{tail} is the tail distance from the head, and $d_{x,y}$ is the distance of a grid cell at x, y location from the head. This resulted in a total of 1,969 linearly interpolated canal point values spaced roughly every 30 m. The estimated canal values were then used with GPI (second-order polynomial equation) to generate MINWTE at 3 m resolution to match the cell alignment of LiDAR DEM. The depth to MINWTE was also created by subtracting MINWTE from LiDAR DEM. The MINWTE and difference between MINWTE and LiDAR DEM were distinguished by physiographic region. With response variable WTE, MINWTE and the difference between MINWTE and LiDAR DEM (depth to MINWTE) were utilized as explanatory variables in both MLR and GWR (adaptive

kernel bandwith using Alkaike Information Criterion) to generate WTEMs for each physiographic region.

Two deterministic approaches (GPI and IDW) and two geostatistical approaches (OK and EBK) were also examined for generating WTEMs. The 35 WTEs and 1,969 canal values were merged and distinguished by physiographic region first. These two datasets were interpolated using the GPI (second-order polynomial equation), IDW (power value of 2), OK (a second order trend was removed before utilizing an anisotropic spherical covariogram model), and EBK (automated adjustments to parameters), respectively. Similarly, 3-m resolutions of WTEMs were generated from these approaches to match the cell alignment of the LiDAR DEM.

The accuracy of the WTEMs derived from the above six approaches was assessed using the randomly selected 30 monitoring points (17 in the Atlantic Coastal Ridge, and 13 in the Southern Slope). The RMSE calculated by the following formula was used to assess the accuracy and determine the best WTEM for the study site:

$$RMSE = \sqrt{\left(Z_{data,\,i} - Z_{check,\,i}\right)^2 \Big/ n} \tag{2}$$

where $Z_{data,i}$ is the estimated water level value, and $Z_{check,i}$ is the observed water level, and n is the number of check points. Once the approach with the best RMSE was identified for each physiographic region, inundation was modeled.

3.2 Modeling groundwater and marine inundation

To model the probability of potential groundwater and marine inundation based on the uncertainty of the underlying data, we considered vertical errors in LiDAR DEM, WTEMs, SLR estimates, transformations, tidal and orthometric datums, and determined their probability distributions. For the LiDAR DEM, we assumed the RMSE of 6.5 cm corresponds to the standard deviation (σ; data follow Gaussian distribution with zero bias). For WTEMs, error statistics were calculated to identify data departures from Gaussian distributions by physiographic region (Table 1). The Atlantic Coastal Ridge data have −2 cm bias, which was corrected by adding 2 cm to the WTEM. However, the skew exceeds ±0.5 indicating errors depart from a Gaussian distribution and are negatively skewed to the left (Table 1). The Southern Slope data have −3 cm bias, which was corrected by adding 3 cm to the WTEM. Additionally, the skew does not exceed ±0.5 indicating errors follow a Gaussian distribution (Table 1). Next, errors in datums, transformations, and future SLR estimates were considered.

It is common in SLR assessment to vertically transfer elevation data to MHHW. However, the study area extends a good length inland from the coast (as much as 25 km). Since the

Table 1 Error statistics for predicted vs. independent water levels used in accuracy assessment

Δ water level observations and predicted								
Physiographic region	RMSE (cm)	μ (cm)	Median (cm)	Skew	σ (cm)	*n*	Min (cm)	Max (cm)
Consolidated	13	1	−1	0.59	13	30	−26	36
Atlantic Coastal Ridge	16	−2	3	−0.7	17	17	−39	20
Southern Slope	6	−3	−4	0.42	6	13	−11	8

Where Δ = difference, *RMSE* = Root Mean Square Error, *n* = number of points, σ = standard deviation, and μ = mean

saltwater intrusion boundary hydraulically connects groundwater and seawater, we assumed areas west of the saltwater intrusion line were not tidally influenced, thus they should not be referenced to a tidal datum. The 250 mg per liter (mg/L) saltwater intrusion line from 1996 obtained from South Florida Information Access (SOFIA) (http://sofia.usgs.gov/exchange/gis/; see Fig. 1) was used to determine whether to vertically reference the LiDAR DEM and WTEMs to NAVD 88 or MHHW. WTEMs and LiDAR DEM west of the saltwater intrusion were kept referenced to NAVD 88 with no transformation. WTEMs and LiDAR DEM east of the saltwater intrusion line were converted to MHHW using VDatum (http://vdatum.noaa.gov/welcome.html) through a process similar to Gesch (2013). The errors associated with each vertical datum and transformation made between them were obtained from NOAA (2013), and shown in Fig. 2. The Cumulative Vertical Uncertainty standard deviation (CVU_σ) is calculated using root sum of squares:

$$CVU_\sigma = \sqrt{\sigma_1^2 + \sigma_2^2 + \ldots \sigma_N^2} \tag{3}$$

for all LiDAR and WTEMs (see Table 2) with one exception. Atlantic Coastal Ridge WTEMs σ were excluded because errors do not follow a Gaussian distribution (see Table 1), thus uncertainty values for these WTEMs were accounted for separately from the CVU_σ. For future SLR estimates, the IPCC AR5 RCP 8.5 scenario median value of 74 cm with likely range (52 to 98) of global SLR by 2100 (Church et al. 2013) was considered. The unknown real distribution of these estimates was formalized in terms of a triangular distribution (Purvis et al. 2008; Cooper and Chen 2013). After determining the vertical errors and probability distributions, inundation was modeled.

Two approaches were employed in Mathworks' MATLAB for mapping inundation. First, a conventional assessment (without WTEM) was utilized to produce a raster that considers no uncertainty in LiDAR and SLR estimates using the following equation:

$$Inundation_{x,y} = SLR > LiDAR_{x,y} \tag{4}$$

where $Inundation_{x,y}$ is a grid cell at x, y location as either 0 (not inundated) or 1 (inundated), SLR is the SLR median of 74 cm, and $LiDAR_{x,y}$ is an elevation value of a grid cell at x,y location. Second, a proposed assessment (with WTEM) was utilized to produce a second raster

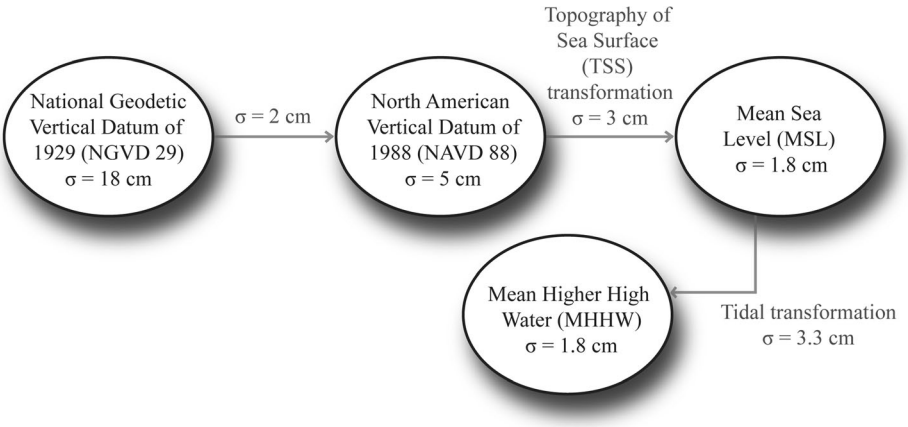

Fig. 2 VDatum vertical errors calculated as standard deviation values for South Florida modified from NOAA (2013). Arrows denote transformation processes, and ovals denote source data

Table 2 Errors from Water Table Elevation (WTEM), LiDAR elevation, datums and transformations between them all expressed as standard deviation (σ) and used to calculate Cumulative Vertical Uncertainty (CVU_σ) for each physiographic region using Eq. 3

Errors				
Elevation type	σ (cm)	Datum/s σ (cm)	Datum Transformation σ (cm)	CVU_σ (cm)
Southern Slope $WTEM_{MHHW}$	6.0	18.9	4.9	20.4
Southern Slope $LiDAR_{MHHW}$	6.5	5.6	4.5	9.7
Southern Slope $WTEM_{NAVD88}$	6.0	18.7	2.0	19.7
Southern Slope $LiDAR_{NAVD88}$	6.5	5.0	–	8.2
Atlantic Coastal Ridge $WTEM_{MHHW}$	–	18.9	4.9	19.5
Atlantic Coastal Ridge $LiDAR_{MHHW}$	6.5	5.6	4.5	9.7
Atlantic Coastal Ridge $WTEM_{NAVD88}$	–	18.7	2	18.8
Atlantic Coastal Ridge $LiDAR_{NAVD88}$	6.5	5.0	–	8.2

Where *MHHW* Mean Higher High Water, and *NAVD 88* North American Vertical Datum of 1988

that considers no uncertainty using the following equation:

$$Inundation_{x,y} = WTEM_{x,y} + SLR > LiDAR_{x,y} \quad (5)$$

where the only difference from Eq. 4 is the addition of $WTEM_{x,y}$, or water table z value of a grid cell at x,y location. Second, Monte Carlo simulation was used to propagate probability distributions through our following three inundation models that consider uncertainty (Eq. 6, 7, 8). First, closely following Cooper and Chen (2013) uncertainty was considered in future SLR estimates, LiDAR DEM, datums and transformation errors for all areas using the following equation:

$$P_{x,y} = \left(SLR_\varepsilon > LiDAR_{CVU_\sigma} + LiDAR_{x,y}\right) \Big/ n \quad (6)$$

where $P_{x,y}$ is the probability of a grid cell at x,y location of being inundated taking a value anywhere from 0 to 1, SLR_ε is a random variable sampled from triangle distribution with a range between 52 and 98 cm and most probable value of 74 cm, $LiDAR_{CVU_\sigma}$ is a random variable sampled from either Gaussian distribution (0, 8.2) for LiDAR referenced to NAVD 88 or (0, 9.7) for LiDAR referenced to MHHW (see Table 2), $LiDAR_{x,y}$ is a constant elevation value of a grid cell at x ,y location, and n is the number of cases we specify. The sampling procedure was repeated 10,000 times for each grid cell, respectively. The following equation was used to consider uncertainty in future SLR estimates, LiDAR DEM, WTEM, datum and transformation errors for the Southern Slope:

$$P_{x,y} = \left(WTEM_{CVU_\sigma} + WTEMx,y + SLR_\varepsilon > LiDAR_{CVU_\sigma} + LiDARx,y\right) \Big/ n \quad (7)$$

where the difference from Eq. 6 is that $WTEM_{CVU_\sigma}$ is a random variable sampled from either Gaussian distribution (0, 19.7) for WTEM referenced to NAVD 88 or (0, 20.4) for WTEM referenced to MHHW (see Table 2), and $WTEM_{x,y}$ is a constant water table z value of a grid cell at x,y location. The following equation was used to consider uncertainty in future SLR estimates, LiDAR DEM, WTEM, datum and transformation errors for the Atlantic Coastal

Ridge because WTEM errors do not follow Gaussian distribution:

$$P_{x,y} = (WTEM_{\varepsilon} + WTEM_{CVU_{\sigma}} + WTEMx,y + SLR_{\varepsilon} > LiDAR_{CVU_{\sigma}} + LiDARx,y) \Big/ n \quad (8)$$

where the difference from Eq. 7 is the addition of $WTEM_{\varepsilon}$, where a random variable is sampled from Gumbel minima (enabling us to model left skewed data) distribution (0, 17) (see Table 1), and $WTEM_{CVU_{\sigma}}$ is a random variable sampled from either Gaussian distribution (0, 18.8) for WTEM referenced to NAVD 88 or (0, 19.5) for WTEM referenced to MHHW (see Table 2). The outputs were six new 3 m resolution rasters where each grid cell contains a probability value anywhere between 0 and 1 of being inundated based on the uncertainty in the underlying data.

The two rasters that did not consider any uncertainty with and without WTEM, and the six probability rasters were used to calculate vulnerable land area. Probability rasters were reclassified using the following ranking scheme: the range of probability values 0.94–1 were reclassified as high probability (>95 %). Areas hydrologically connected to the ocean (groundwater and direct marine inundation) were not distinguished differently from areas not hydrologically connected to the ocean (groundwater inundation). The eight polygon layers were then used to calculate vulnerable land area to determine the effect of considering WTEM with and without uncertainty.

4 Results and discussion

4.1 Water Table Elevation Model (WTEM) vertical accuracy

The evaluation of several deterministic and geostatistical methods used for generating WTEM found that IDW gave the best result (e.g., Varouchakis and Hristopulos 2012). However, for our study site IDW presented a poor result in producing the WTEM (Table 3). Kriging was widely used to estimate groundwater levels (e.g., Desbarats et al. 2001; Zhu et al. 2013). Compared to IDW, Kriging produced a better RMSE, which is consistent with the result from Yao et al. (2014). OK and EBK reduced the RMSE slightly compared to the IDW for Atlantic Coastal Ridge, and EBK resulted in the best RMSE for Southern Slope in this study (Table 3). The use of statistical methods such as MLR was also employed to estimate WTEM (Sepulveda 2003). In this study, MLR provided the worst RMSE for both physiographic regions (Table 3).

Table 3 The Root Mean Square Errors (RMSEs) of six tested approaches for generating Water Table Elevation Model (WTEM) in two physiographic regions. Two identified approaches are in bold

Approach	Atlantic Coastal Ridge		Southern Slope	
	RMSE (cm)	R^2	RMSE (cm)	R^2
Global Polynomial Interpolation (GPI)	**16**		10	
Empirical Bayesian Kriging (EBK)	18		**6**	
Ordinary Kriging (OK)	18		7	
Inverse Distance Weighting (IDW)	19		8	
Geographic Weighted Regression (GWR)	18	0.93	8	0.72
Multiple Linear Regression (MLR)	20	0.90	11	0.66

In comparing MLR to GWR, GWR provided a better RMSE and higher coefficient of multiple determinations (R^2) for both physiographic regions (Table 3). In another study, a WTEM derived from GPI gave a better RMSE when compared to Kriging (Yao et al. 2014). In this study, GPI yielded the best result with the lowest RMSE for Atlantic Coastal Ridge (Table 3). Therefore, WTEM generated from GPI was used for Atlantic Coastal Ridge, and WTEM derived from EBK was used for Southern Slope. These results show the importance to testing different approaches used for generating WTEM in order to reduce uncertainty.

4.2 Effect of no uncertainty with WTEM on vulnerable land area

Direct marine inundation was often mapped in a GIS by identifying areas hydrologically connected to the ocean because it was assumed that inland areas will not flood (e.g., Poulter and Halpin 2008). On the other hand, areas hydrologically disconnected from the ocean were also mapped in previous studies because it was assumed these areas will experience groundwater inundation (although WTEM was excluded; Cooper et al. 2012; Cooper and Chen 2013; Kane et al. 2014). In this study, models that excluded uncertainty without WTEM resulted in land area for both types of inundation to be consistently underestimated regardless of physiographic region and vertical reference system (Table 4). Total land area flooded was 51.3 % of the SLR study area when excluding uncertainty without WTEM and 58.9 % when excluding uncertainty with WTEM (Table 4). Thus, excluding uncertainty without WTEM resulted in a difference of −14 % in total land area inundated. If WTEM and uncertainty are going to be excluded, it is better to map both areas connected to and disconnected from the ocean to prevent further potential underestimation of vulnerable land area. However, these results together with Rotzoll and Fletcher (2012) and Marrack (2014) show it is best to include WTEM when excluding uncertainty.

Table 4 Vulnerable area to sea-level rise (SLR) with and without uncertainty

			Uncertainty excluded: LiDAR, SLR estimates		Uncertainty excluded: LiDAR, SLR estimates, WTEM		Uncertainty included: LiDAR, SLR estimates, datums & their transformations		Uncertainty included: LiDAR, SLR estimates, datums & their transformations, WTEM	
	High confidence (P>95 %)									
Physiographic region	Area (km^2)	% study area	Area (km^2)	% study area	Area (km^2)	% study area	Area (km^2)	% study area	Area (km^2)	% study area
Atlantic Coastal $Ridge_{NAVD88}$	61.12	37.70	7.04	4.34	12.73	7.85	5.18	3.19	4.77	2.94
Atlantic Coastal $Ridge_{MHHW}$	8.88	5.48	4.52	2.79	4.75	2.93	3.65	2.25	0.97	0.60
Southern $Slope_{NAVD88}$	35.18	21.70	19.75	12.18	24.89	15.35	16.24	10.02	11.36	7.01
Southern $Slope_{MHHW}$	56.96	35.13	51.94	32.03	53.13	32.77	48.27	29.77	45.39	27.99
Σ	162.14	100.00	83.25	51.34	95.50	58.90	73.34	45.23	62.49	38.54

Where *WTEM* = Water Table Elevation Model, and Σ = sum

4.3 Effect of uncertainty with WTEM on vulnerable land area

Recently, studies are incorporating WTEM into the inundation modeling because it is understood land area is underestimated when excluding WTEM (e.g., Rotzoll and Fletcher 2012; Manda et al. 2014) and as also demonstrated in section 4.2 of this study. However, the effect of excluding uncertainty in WTEM is still not well understood. In this study, excluding WTEM with uncertainty at the 95 % probability threshold resulted in total land area consistently overestimated regardless of physiographic region, vertical reference system, and probability density function used to include error in WTEM (Table 4). Total land area flooded was 45.23 % of the SLR study area when excluding WTEM with uncertainty and 38.54 % when including WTEM with uncertainty (Table 4). Thus, excluding WTEM with uncertainty resulted in a difference of +16 % in total land area inundated at the 95 % probability threshold. We note how the probability threshold is defined determines the magnitude in difference between vulnerable land areas. For this reason, we did not compare vulnerable land area between models that either exclude or include uncertainty from section 3.2 and in Table 4. Overall, in order to reduce error in the marine and groundwater inundation modeling, these results show the uncertainty in the WTEM should be considered.

The SLR vulnerability map that considers uncertainty in future SLR estimates, LiDAR elevation, tidal and orthometric datums, transformations, and groundwater modeling derived from EBK for Southern Slope (using Eq. 7) and GPI for Atlantic Coastal Ridge (using Eq. 8) is shown in Fig. 3. Homestead Air Reserve Base will be adversely impacted by inundation and drainage problems accompanied by rise of the water table. Turkey Point Nuclear Generating Station facility will be flooded affecting South Florida's energy and electricity users if no adaptation strategies are taken. Open water areas in both Homestead and Florida City will expand due to rise of the water table, which is accompanied by saltwater intrusion through the ground. The majority of inundated area is estuarine and palustrine wetland, where palustrine wetlands will likely change to estuarine depending on the capacity of mangrove soils to increase in elevation with the rate of SLR. Although the collection of sediment cores for measuring

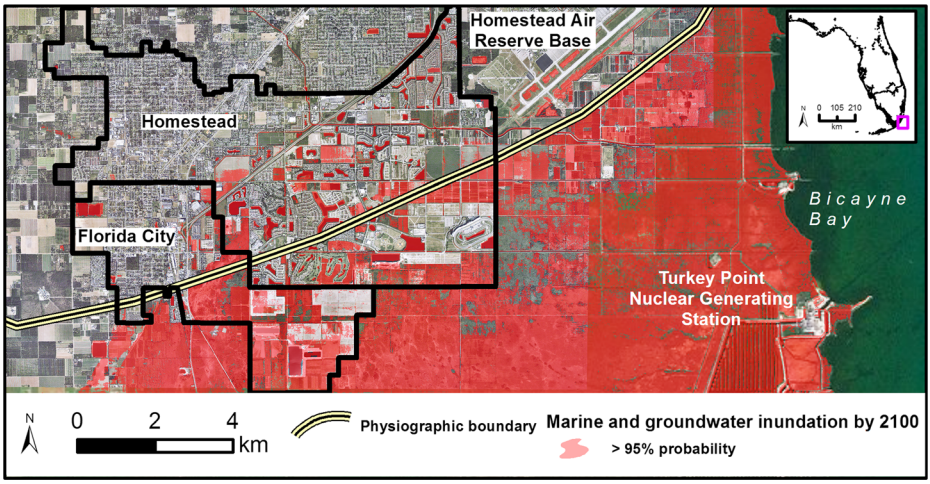

Fig. 3 SLR vulnerability map including uncertainty in SLR estimates, LiDAR, vertical datums, transformations, and groundwater modeling highlighting lands vulnerable under SLR of 74 cm with range between 52 and 98 by year 2100 for the two most southern cities in mainland Florida

marsh accretion rates is beyond the scope of this study, it is likely that marsh areas are slightly overestimated because we do not consider accretion rates along with their uncertainty.

5 Conclusions

In this study we evaluated the effects of four scenarios when assessing land area vulnerable to marine and groundwater inundation in South Florida. First, we examined different approaches to generating Water Table Elevation Model (WTEM) and identified models with the best vertical accuracy. Second, we compared vulnerable land area assessed from two simple inundation models that consider no uncertainty with and without Water Table Elevation Model (WTEM). Third, we compared vulnerable land area at >95 % confidence assessed from two refined inundation models using the Monte Carlo approach that considers uncertainty in future SLR estimates, LiDAR DEM, vertical datums and transformations made between them with and without WTEM uncertainty. We identified the following:

- Empirical Bayesian Kriging (EBK) resulted in the best RMSE for Southern Slope, while Global Polynomial Interpolation (GPI) yielded the best RMSE for Atlantic Coastal Ridge. It is important to test different approaches in order to reduce uncertainty in WTEM.
- Excluding uncertainty without WTEM resulted in total land area inundated to be underestimated by 14 % when compared to excluding uncertainty with WTEM. If WTEM and uncertainty are going to be excluded, it is better to map both areas connected to and disconnected from the ocean to prevent further potential underestimation of vulnerable land area. However, it is best to incorporate the WTEM when not considering uncertainty.
- Including uncertainty in SLR estimates, LiDAR DEM, vertical datums and transformations made between them when excluding WTEM with uncertainty at >95 % confidence resulted in total land area to be overestimated by 16 % when compared to including WTEM with uncertainty. Including WTEM with uncertainty adds to the integrity of the SLR mapping tools and should be considered so that more effective adaptation decisions can be made.

This paper is expected to extend vulnerability mapping to include uncertainty in groundwater modeling. Continuing research includes the error in models that use three-dimensional finite difference groundwater models such as the USGS MODFLOW (McDonald and Harbaugh 1988) to simulate groundwater levels in response to SLR. This would allow for the comparison of how well including error in WTEM is used to assess vulnerability to groundwater inundation. Including uncertainty in marsh migration and accretion is also important to compare with WTEM's ability to capture (or not capture) groundwater inundation. Overall, Monte Carlo simulation is a valuable approach to addressing uncertainty in vulnerability mapping regardless of error distribution.

Acknowledgments We thank Jorge Restrepo, Angela Montoya, Leonard Berry and Florida Center for Environmental Studies, Qi Chen, Charles Fletcher, Matthew Barbee, Haunani Kane and Hawai'i Coastal Geology Group, Ev Wingert, Matthew McGranaghan, Virginia Walsh, Tim Liebermann, Tobin Hindle, Keren Bolter, and our three anonymous reviewers.

References

Chung J, Rogers JD (2012) Interpolations of groundwater table elevation in dissected uplands. Groundw 50:598–607

Church JA et al (2013) Sea Level Change. In: Climate Change 2012: The Physical Science Basis. Contribution of Working Group 1 to the Fifth Assessment of the Intergovernmental Panal on Climate Change. [Stocker, TF, D Qin, G –K Plattner, M Tignor, S K Allen, J Boschung, A Nauels, Y Xia, V Bex and P M Midgley (eds)]. Cambridge University Press, Cambridge, United Kingdom and New York, NY, USA

Cooper HM, Chen Q (2013) Incorporating uncertainty of future sea-level rise estimates into vulnerability assessment: A case study in Kahului. Maui Clim Change 121:635–647

Cooper HM, Chen Q, Fletcher C, Barbee M (2012) Vulnerability assessment due to sea-level rise in Maui, Hawaíi using LiDAR remote sensing and GIS. Clim Change 116:547–563

Cooper HM, Fletcher C, Chen Q, Barbee M (2013) Sea-level rise vulnerability mapping for adaptation decisions using LiDAR DEMs. Prog Phys Geog 37:745–766

Desbarats AJ, Logan CE, Hinton MJ, Sharpe DR (2001) On the kriging of water table elevations using collateral information from a digital elevation model. J Hydrol 255:25–38

FGDC (1998) Geospatial positioning accuracy standards, Part 3. National Standard for Spatial Data Accuracy. FGDC-STD-007.3-1998, http://www.fgdc.gov/standards/projects/FGDCstandardsprojects/accuracy/part3/index_html. Accessed 26 Mar 2014

Fish JE, Stewart M (1991) Hydrogeology of the surficial aquifer system Dade County, Florida. U.S. Geological survey water-resources investigations report 90–4108. Available at: http://sofia.usgs.gov/publications/wri/90-4108/wri904108.pdf. Assessed 6 Dec 2014

Fotheringham AS, Charlton ME, Brunsdon C (1998) Geographcially weighted regression, a natural evolution of the expansion method for spatial data analysis. Environ and Plan A 30:1905–1927

Gesch D (2009) Analysis of Lidar elevation data for improved identification and delineation of lands vulnerable to sea-level rise. J Coastal Res 53:49–58

Gesch D (2013) Consideration of vertical uncertainty in elevation-based sea-level rise assessments: Mobile Bay, Alabama case study. J Coastal Res 63:197–210

Giddings JB, Kuebler LL, Restrepo JI, Rodberg KA, Montoya AM, Radin HA (2006) Lower east coast subregional (LECsR) MODFLOW model documentation. Available at: http://www.sfwmd.gov/portal/page/portal/xrepository/sfwmd_repository_pdf/lec_sr_draft_documentation.pdf. Accessed 4 Dec 2014

Kane HH, Fletcher CH, Frazer LN, Barbee MM (2014) Critical elevation levels for flooding due to sea-level rise in Hawaíi. Reg Environ Change. doi:10.1007/s10113-014-0725-6

Leon JX, Heuvelink GBM, Phinn SR (2014) Incorporating DEM uncertainty in coastal inundation mapping. PLoS One. doi:10.1371/journal.pone.0108727

Manda AK, Sisco MS, Mallinson DJ, Griffen MT (2014) Relative role and extent of marine and groundwater inundation on a dune-dominated barrier island under sea-level rise scenarios. Hydrol. Process. In press

Marrack L (2014) Incorporating groundwater levels into sea level detection models for Hawaiian anchialine pool ecosystems. J Coastal Res. In press

Masterson JP, Fienen MN, Thieler ER, Gesch DB, Guitierrez BT, Plant NG (2013) Effects of sea-level rise on barrier island groundwater system dynamics – echohydrological implications. Echohydrology 7:1064–1071

McDonald MG, Harbaugh AW (1988) A modular three-dimensional finite-difference groundwater flow model: Techniques of water-resources investigations of the US Geological Survey. Book 6, US Government Printing Office, Washington, DC

Mitsova D, Esnard A, Li Y (2012) Using dasymteric mapping techniques to improve the spatial accuracy of sea level rise vulnerability assessments. J Coast Conservat 16:355–372

National Digital Elevation Program (NDEP) (2004) Guidelines for digital elevation data, Version 1.0. Available at: www.ndep.gov/NDEP_Elevation_Guidelines_Ver1_10May2004.pdf. Accessed 17 Mar 2014

NOAA (2013) VDatum. http://vdatum.noaa.gov/docs/est_uncertainties.html. Assessed 16 Aug 2014

Poulter B, Halpin P (2008) Raster modeling of coastal flooding from sea-level rise. Int J Geogr Inf Sci 22:168–182

Purvis M, Bates P, Hayes C (2008) A probabilistic methodology to estimate future coastal flood risk due to sea level rise. Coast Eng 55:1062–1073

Qian SS (1997) Estimating the area affected by phosphorous runoff in an Everglades wetland: a comparison of universal kriging and Bayesian kriging. Environ Ecol Stat 4:1–29

Rotzoll K, Fletcher C (2012) Assessment of groundwater inundation as a consequence of sea-level rise. Nat Clim Change 3:477–481

Schmid K, Hadley BC, Wijekoon N (2011) Vertical accuracy and use of topographic LiDAR data in coastal marshes. J Coastal Res 27:116–132

Schmid K, Hadley B, Waters K (2013) Mapping and portraying inundation uncertainty of bathtub-type models. J Coastal Res 30:548–561

Sepulveda N (2003) A statistical estimator of the spatial distribution of the water-table altitude. Groundw 41:66–71

SFWMD (2014) Canals in South Florida: a technical support document. Available at: http://www.sfwmd.gov/portal/page/portal/xrepository/sfwmd_repository_pdf/canalssfl_appendixa-c.pdf. Assessed 10 Dec 2014

Sun Y, Kang S, Li F, Zhang L (2009) Comparison of interpolation methods for depth to groundwater and its temporal and spatial variations in the Minqin oasis of northwest China. Environ Model Softw 24:1163–1170

Varouchakis EA, Hristopulos DT (2012) Comparison of stochastic and deterministic methods for mapping groundwater level spatial variability in sparsely monitored basins. Environ Monit Assess 185:1–19

White WA (1970) The geomorphology of the Florida Peninsula. Florida Geol Surv Bull 51:1–164

Yao L, Huo Z, Feng S, Mao X, Kang S, Chen J, Xu J, Steenhuis TS (2014) Evaluation of spatial interpolation methods for groundwater level in an arid inland oasis, northwest China. Environ Earth Sci 71:1911–1924

Zhu K, Cui Z, Jiang B, Yang G, Chen Z, Meng Q, Yao Y (2013) A DEM-based residual kriging model for estimating groundwater levels within a large-scale domain: a study for the Fuyang River Basin. Clean Techn Environ Policy 15:687–698